Iran University of Science and Technology
Iranian Journal of Electrical and Electronic Engineering
Journal Homepage: ijeee.iust.ac.ir

A Wideband Circularly Polarized L/S Septum Horn Feed for Portable Satellite Communication

Amir M. Zaker*, Mohammad Bod*(C.A.) and Hamid G. Bafghi**

Abstract: This paper proposes a novel wideband circularly polarized L/S feed system for portable satellite communications. The feed system integrates a multi-stage septum polarizer, a sloped waveguide transition, and an axial choke conical horn to ensure uniform reflector illumination of a 3-meter reflector antenna. Unlike existing septum-based feed designs, the proposed structure achieves an ultra-wide 47% fractional bandwidth (1.6–2.6 GHz) with an axial ratio below 2 dB. It is explicitly optimized for use as a reflector feed rather than as a standalone antenna. A foldable multi-piece strut mechanism is introduced to enhance portability and facilitate field deployment. In addition, a convex plate at the reflector vertex is employed to reduce feed blockage and improve gain, particularly at higher frequencies. Simulation and measurement results are compared, demonstrating superior performance of the proposed antenna to existing solutions, including high isolation (>15 dB) between ports and sidelobe levels better than 26 dB. The combination of wideband circular polarization, reflector-level optimization, and mechanical portability distinguishes this work from prior septum-horn and portable reflector-antenna solutions.

Keywords: Satellite communication, circular polarization, septum polarizer, corrugated horn, reflector antenna, wideband antenna, portable ground station.

1 Introduction

In recent years, satellite communication systems have been increasingly used for various applications, including broadcasting, telecommunications, and remote sensing. Satellite communications have revolutionized connecting and sharing information over vast distances [1]. The ability to transmit data wirelessly over long distances has made satellite communications an essential tool in our interconnected world. This growing demand has intensified the need for portable ground station antennas capable of operating across multiple frequency bands while maintaining high performance in challenging environments [2].

Reflector antennas are the dominant configuration for most of the satellite ground stations [3]. This type of antenna is of interest because of its high gain and directional characteristics. Different types of reflector antennas, such as Cassegrain antennas [4], Gregorian antennas [5], offset parabolic antennas [6], hat-feeds [7], [8], and self-supported feeds [9], are widely proposed in the literature for satellite communication.

Among these configurations, prime focus reflector antennas are particularly well-suited for portable applications because of their simple feed alignment and high efficiency [10]–[14]. The performance of this antenna depends on the feed antenna design, which must provide uniform illumination of the reflector while maintaining excellent polarization purity across the operating band. Traditional feed solutions often struggle to simultaneously meet the requirements for wide bandwidth and compact size.

Iranian Journal of Electrical & Electronic Engineering,
Paper first received and accepted.
* The authors are with the Department of Electrical Engineering Shahid Rajaee Teacher Training University, Tehran, Iran.
E-mail: amirmzaker@sru.ac.ir, Mohammadbod@sru.ac.ir
** The authors is with the Department of Electrical Engineering, Sharif University of Technology, Tehran, Iran.
E-mails: h.bafghi@staff.sharif.edu
Corresponding Author: mohammad bod

In satellite communication, circular polarization (CP) is highly advantageous due to its ability to mitigate signal degradation effects caused by multipath propagation and atmospheric interference. Circular polarization maintains consistent signal integrity regardless of the orientation of the receiving antenna. This characteristic is particularly beneficial in dynamic environments where the satellite's position may vary due to orbital motion or when the ground station is portable [15]–[18].

A review and comparison of the different designs of circularly polarized (CP) antennas is presented in [15]. In [17], a broadband circularly polarized C-shaped slot antenna for L/S-band applications was designed. Although the authors also created a 2×2 array with sequential rotation feeding, which demonstrated improved gain (13.4 dBic), this gain is lower than the requirement of most satellite communication systems. In [18], a wideband dual-circularly polarized inverted quad-ridged elliptical waveguide horn antenna that achieves a 66.7% bandwidth (4–8 GHz) was designed. Although dual-polarized designs such as the quad-ridged horn in [18] report a wider fractional bandwidth of 66.7%, they rely on asymmetric elliptical apertures that produce elliptical radiation patterns. These non-rotational profiles cause severe edge-spillover and highly non-uniform illumination when applied to circular prime-focus dishes. The feed proposed in this work deliberately optimizes the fractional bandwidth to 47% while strictly maintaining a rotationally symmetric hybrid HE_{11} mode through integrated axial chokes. This specific boundary control ensures uniform reflector illumination and preserves a system aperture efficiency above 60% across the operating frequency band.

Septum polarizers have emerged as a promising solution for circular polarization generation in compact feed systems [19]–[30]. These devices integrate the polarization conversion function directly within the waveguide structure, eliminating the need for bulky external orthomode transducers. The septum polarizer's inherent broadband characteristics make it especially attractive for wideband applications. When combined with properly designed horn antennas, these polarizers can achieve excellent circular polarization performance while maintaining a compact form factor suitable for portable systems.

Recent advances in septum polarizer design have demonstrated their effectiveness in various frequency bands. In [24], a 3D-printed circularly polarized horn antenna with an integrated dielectric septum was designed. This antenna has only 16.7% axial ratio (AR) bandwidth (13.72–16.22 GHz) and 16.44 dBi peak gain at 15 GHz. Another Wideband Dual-Circular-Polarization septum Horn was proposed in [25]. The fabricated antenna shows 21% relative bandwidth with an axial ratio less than 5.8 dB. An X-Band septum horn antenna with a metamaterial lens, which operates over a frequency range of 7-9 GHz with less than 25% relative bandwidth, was proposed in [27].

Despite significant progress in circularly polarized feed antennas, most existing L/S-band feed systems suffer from limited axial-ratio bandwidth, are primarily designed as standalone antennas rather than reflector feeds, and lack mechanical structures suitable for portable ground-station deployment. Furthermore, the combined electrical and mechanical integration of wideband septum feeds with reflector-level performance enhancement has not been sufficiently addressed in prior works, motivating the proposed design.

This paper introduces a wideband circularly polarized feed system for L/S-band satellite communications that addresses these challenges through innovative design approaches. The feed system integrates a multi-stage septum polarizer, a sloped waveguide transition, and an axial choke conical horn to illuminate a 3-meter reflector antenna. The feed horn design incorporates carefully engineered corrugation to improve aperture efficiency, while the multi-stage septum polarizer provides wideband circular polarization with minimal axial ratio variation.

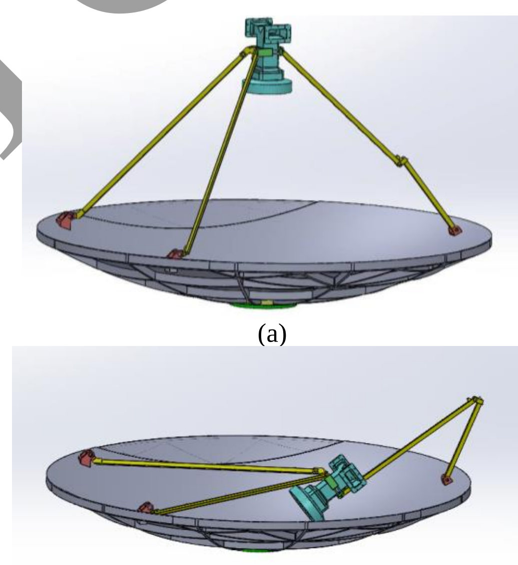

(a)

(b)

Fig. 1. The configuration of the proposed L/S Septum feed reflector antenna for portable satellite communication, (a) antenna at the service, (b) the folded antenna for transporting.

Through detailed simulation and experimental validation, we demonstrate that the proposed design achieves superior performance compared to existing solutions. The antenna maintains an axial ratio better than 2 dB across the 1.6 to 2.6 GHz frequency range (a 47% fractional bandwidth) while exhibiting excellent impedance matching and radiation characteristics. The parabolic reflector antenna has efficiency exceeding 60%

and sidelobe levels better than 26 dB. We have also proposed multi-piece struts to hold the feed at the focal point and fold it up for transportation, making the antenna portable.

The remainder of this paper is organized as follows: Section 2 describes the antenna design methodology in detail, including the corrugated horn and septum polarizer optimization process. Section 3 presents the simulation and measurement results, comparing the antenna's performance with theoretical predictions and existing designs. Finally, Section 4 summarizes the key findings and discusses potential applications of the proposed design.

2 Antenna Design

The configuration of the proposed L/S Septum feed reflector antenna for portable satellite communication is shown in Fig. 1. The proposed antenna consists of a 3-meter reflector, a corrugated conical feed horn, a septum waveguide polarizer, and multi-piece struts. The antenna design is such that during transportation, the multi-piece strut mechanism folds, allowing the feed assembly to be stowed against the reflector surface, as shown in Fig. 1 (b). The foldable tripod mechanism enables field-portable deployment. The design specifications of the proposed antenna are given in Table 1. Next, we will examine the design of each of the antenna sub-sections.

Table 1. The design Specification of the proposed dual-band dual-polarized reflector antenna.

Parameter	Value
Antenna Type	Portable prime focus reflector antenna
Frequency	L/S band 1600-2300MHz
Reflector Diameter	3 meters
Required Axial Ratio	<3dB
Antenna Gain	32dB @ L band, 34 dB@ S band
Antenna Polarization	Dual polarization RHCP and LHCP
S_{11}	<-10dB

2.1 Waveguide septum Polarizer

The configuration of the antenna feed is shown in Fig. 2. As can be seen, the feed has a dual WR510 waveguide port attached to a septum polarizer. Unlike conventional septum polarizers, we eliminated the coaxial adapters in this design and placed two waveguide slots on both sides of the septum. The dimensions of these slots were chosen for the best bandwidth. We then used a pyramidal transition to bring the optimal slot dimensions to the WR510 adapter. Such a design will significantly improve the septum polarized bandwidth and create circular polarization over a wide frequency range.

The septum polarizer can be modeled as an ideal lossless component. If we consider the output port of the polarizer at the antenna side to be two separate ports 3 and 4 (for two different modes), and the input port of the polarizer as ports 1 and 2 (WR510 side), the S-parameter of this structure should be as follows [31] :

$$S_{ij} = \frac{1}{\sqrt{2}} \begin{pmatrix} 0 & 0 & 1 & -j \\ 0 & 0 & -j & 1 \\ 1 & -j & 0 & 0 \\ -j & 1 & 0 & 0 \end{pmatrix} \qquad (1)$$

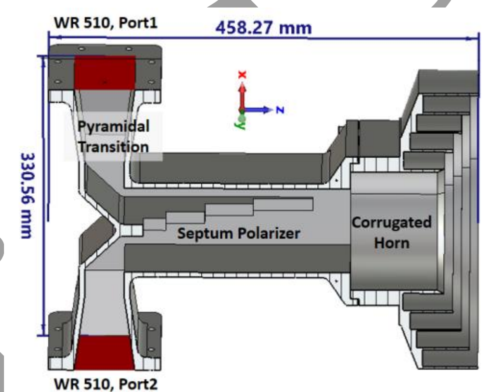

Fig. 2. The broadband Septum Polarizer with the conical corrugated feed horn antenna.

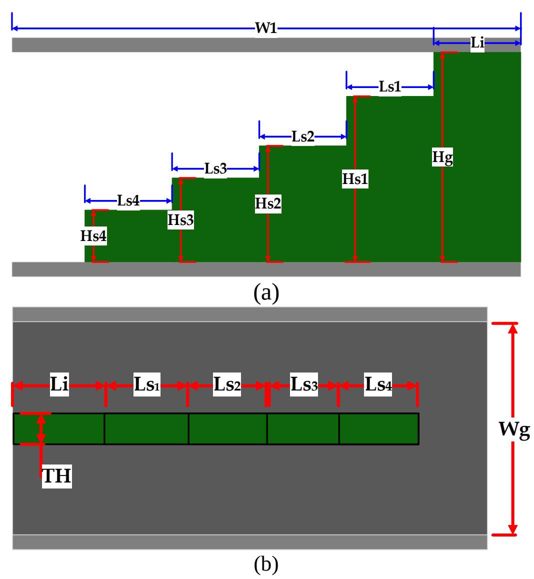

Fig. 3. Design parameters of the proposed Septum Polarizer, (a) side view, (b) top view.

Based on this equation, the ideal septum polarizer should exhibit zero reflection at Ports 1 and 2 and perfect isolation between them while maintaining RHCP radiation (with phase-shifted modes) for Port 1 and LHCP for Port 2.

This work presents a septum polarizer of 5 steps. as shown in Fig. 2, the dimensions of which are initially selected based on theoretical guidelines derived from [32] and subsequently fine-tuned through parametric optimization available in CST Studio Suite®. To meet the target axial ratio (AR) of less than 3 dB for the final antenna system, the optimization goals for the septum and feed subsystems are set more stringently.

Key geometric parameters (segment lengths, widths, and thicknesses, as illustrated in Fig. 3) are optimized using a genetic algorithm (GA) due to the high dimensionality of the design space. The GA employed a population size of 64, a maximum of 40 iterations, a crossover rate of 70%, and a mutation rate of 10%. Tournament selection with a tournament size of 20% was used to balance exploration and exploitation. The GA fitness function was defined over the 1.6-2.6 GHz band as a weighted sum of the input reflection coefficient, and boresight axial ratio, with increased emphasis on polarization performance. The objective function is expressed as:

$$F = \sum_{f \in \mathrm{F}} \left(w_{11} |S_{11}(f)| + w_{22} |S_{22}(f)| + w_{AR} AR(f) \right) \quad (2)$$

Where F $\in [1.6, 2.6]$ GHz denotes the set of sampled frequency points. w_{11}, w_{22} and w_{21} are set to 1, while $w_{AR} = 2$ to assign higher priority to axial-ratio minimization during the optimization process. This formulation ensured broadband circular polarization performance while preserving good matching characteristics.

The final obtained parameters are shown in Table 2.

Table 2. Optimized septum polarizer parameters

Param.	Value	Param.	Value	Param.	Value
HG[a]	98.9	**Ls1**	23.83	**Hs1**	55.32
WG	98.9	**Ls2**	41.75	**Hs2**	38.24
LI	29.79	**Ls3**	51.61	**Hs3**	17.69
TH	13.76	**Ls4**	63.68	**Hs4**	5

[a] Values are in millimeters

Table 3. Optimized parameters for conical horn feed

Param.	Value	Param.	Value
Wd[a]	80.05[a]	**Wr1**	5.37
Ws	19.51	**Wr2**	4.37
Ds1	35.466	**Wr3**	3.87
Ds(2:5)	34.53	**Wr4**	3.37
θ	24.98	**Wr5**	3.37

[a] Values are in millimeters

2.2 Axial Choke Conical Horn Feed

An Axial Choke Conical Horn antenna is used to illuminate the reflector surface uniformly. The axial choke conical horn can illuminate the reflector surface more uniformly due to the creation of the HE_{11} hybrid mode at the antenna aperture [33], which increases the overall efficiency of the reflector antenna. The feed antenna parameters are selected so the feed pattern illuminates the reflector with a 12 dB edge taper.

The parameters of the proposed axial choke horn antenna are selected based on the procedure presented in [33]. As shown in Fig. 4, the most important antenna parameters are Waveguide Diameter (Wd), Flare Angle (θ), Sloth Width (Ws), Slot Depths ($Ds_{1:4}$), and Ridge Widths ($Wr_{1:5}$).

In this antenna, while a wider flare angle can provide higher beam gain due to increased aperture size, a proper decrease in flare angle and beam width can ensure minimum spill-over from reflector edges. The feed parameters alone are optimized for maximum efficiency and the lowest sidelobe, and the results of this optimization are given in Table 3.

2.3 Parabolic Reflector

The designed feed antenna is placed in front of a 3-meter prime focus reflector, as shown in Fig. 1. The designed reflector is made of carbon-coated fiberglass. Such a structure will create a very low weight. The phase center of the designed feed is located at the reflector's focal point with the help of a multi-piece tripod structure. The antenna is designed so that the holder is folded during transportation and the feed is placed on the reflector. Also, the two sides of the reflector structure are considered to be magnetically detachable so that the dimensions of the reflector reach about 2.4 meters during transportation. This mechanism is shown in Fig. 5.

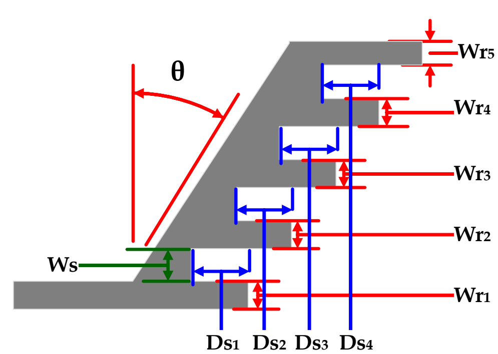

Fig. 4. Design parameters of the proposed Axial Choke Conical Horn Feed

Prime focus reflectors are very suitable structures in terms of the low side lobe area because they illuminate the reflector surface completely uniformly in all directions. However, prime-focus antennas inherently suffer from feed blockage, which reduces gain and aperture efficiency. A convex plate is incorporated at the reflector vertex to redirect blocked rays. According to [8], the introduction of a shaped plate near the reflector vertex can mitigate undesired field interactions, such as multiple reflections, in reflector-fed antenna systems. Motivated by this concept, a convex plate is integrated in the proposed design to improve the electromagnetic behavior of the reflector system. In the proposed design, as shown in Fig. 5, the convex plate redirects a portion of the feed radiation that would otherwise be blocked. This effect becomes more pronounced at higher frequencies, where the feed radiation is more directive and blockage effects are more severe.

Table 4 summarized the main reflector parameters, including the convex plate. The complete design and optimization workflow, including requirement definition, initial geometry synthesis, and GA-assisted refinement of septum and horn parameters, is summarized in Table 5.

Table 4. Reflector parameters

Param.	Value	Param.	Value
Reflector Radius	3000mm	Reflector F/D	0.45
Cone Height	78mm	Cone Radius	320

[a] Values are in millimeters

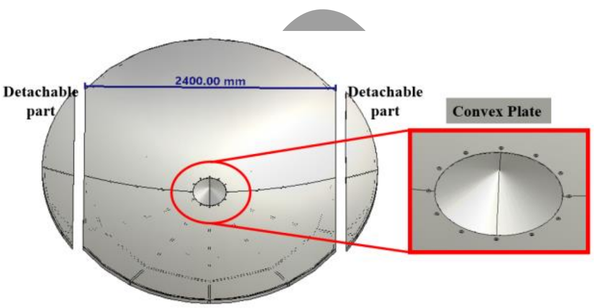

Fig. 5. Adding a convex plate at the vertex of the reflector antenna.

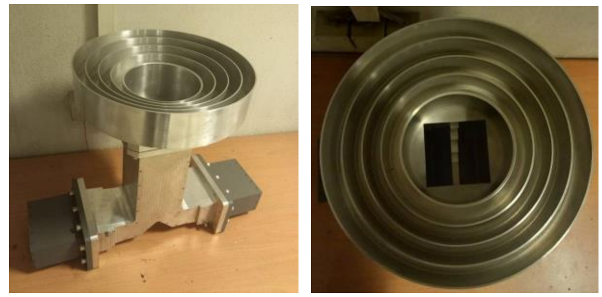

(a) (b)

Fig. 6. Fabricated prototype of the proposed feed antenna with two WR510 adapters; (a) side view, (b) top view.

Table 5. Design procedure of the L/S-band reflector antenna

Inputs	Reflector Geometry parameters from Table 4.
Step 1:	**Reflector-driven horn synthesis**
1.1	Build the prime-focus reflector model and extract the rim subtended angle from the geometry using the feed reference point. Rim angle ≈ 47° (geometry).
1.2	Define the horn radiation requirement such that the field level at the rim angle is approximately −12 dB.
Step2:	**Design the horn antenna with $\approx -12dB$ taper @ 47°rim angle**
2.1	Initialize horn flare angle, length, aperture, choke depth, and corrugation parameters using standard corrugated horn guidelines [33].
2.2	Optimize the standalone horn to achieve stable radiation patterns and acceptable impedance matching over the operating band.
2.3	Integrate the horn with the reflector and refine horn parameters to satisfy taper, gain stability, and sidelobe requirements.
Step3:	**Septum polarizer design and optimization**
3.1	Model the septum as a three-port structure with the circular input as Port 3 and rectangular outputs as Ports 1 and 2.
3.2	Initialize septum step dimensions using standard stepped-septum design guidelines.
3.3	Optimize septum geometry to achieve good matching at the circular input, $\lvert S_{31}\rvert \approx -3dB$ power split, adequate isolation, and axial ratio performance.
Step4:	**Integrated feed verification**
4.1	Integrate the optimized septum with the horn and evaluate the structure as a two-port feed.
4.2	Verify impedance matching, axial ratio, and radiation pattern stability of the integrated feed.
Step5	**Full system validation**
5.1	Integrate the feed with the reflector and simulate system-level performance.
5.2	Confirm compliance with the requirement table.

5.3	Fabricate the feed and validate simulated results through measurements.
Outputs	Final optimized geometry based on the Goal of Table 1.

3 Simulations and Measurements

This section discusses the simulation results of each component. All electromagnetic simulations were performed in CST Studio Suite using Frequency Solver (for septum-feed structure) and Integral Equation Solver (for reflector-integrated structure). Waveguide ports were assigned at the inputs of the septum to excite the fundamental mode, and open (add space) boundary conditions were applied around the horn aperture to emulate free-space radiation. An adaptive mesh refinement process is applied to the frequency solver simulations, with additional refinements around the septum steps, the waveguide transitions and the horn aperture to ensure convergence of S-parameters and axial-ratio predictions across the L/S band.

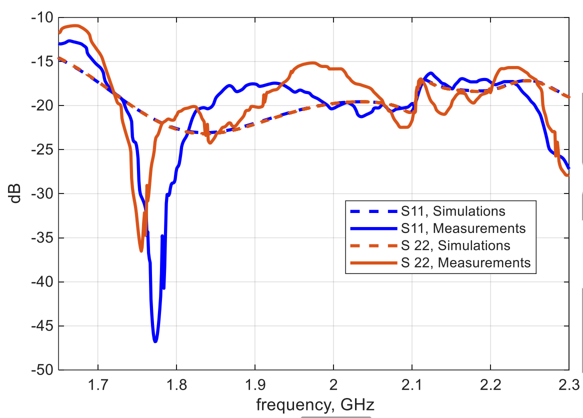

Fig. 7. The simulated and measured S-parameter of the proposed septum horn feed antenna.

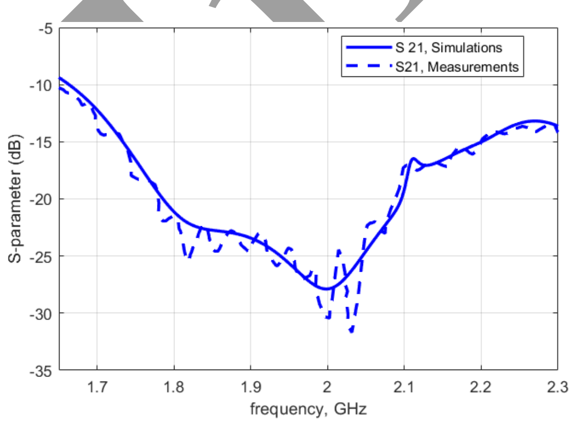

Fig. 8. The simulated and measured S_{21} (Isolation) of the proposed septum horn feed antenna.

A prototype of the proposed septum feed horn antenna was fabricated as shown in Fig. 6. The S-parameter (S_{11}, S_{22}) of this antenna is measured and compared with the simulation results, as shown in Fig. 7 and Fig. 8. Fig. 7 compares the simulation results of S_{11} and S_{22} at the antenna ports with the measurement results. As demonstrated in both the measurement and simulation results, the antenna has a return loss better than 10 dB in the range of 1.6 to 2.3 GHz. In this figure in the simulation result, the S_{11} and S_{22} parameters are completely consistent, which is due to the ideality and symmetry of the structure, but in the measurement result, a slight deviation between these two parameters is observed.

The RHCP and LHCP radiation patterns of the feed antenna are shown in Fig. 9. This figure plots the RHCP and LHCP patterns for both antenna ports at frequencies of 1.65, 2, and 2.3 GHz. As can be seen, the RHCP pattern dominates in the first port, while the LHCP pattern dominates in the second port. The patterns also demonstrate uniform reflector illumination without additional sidelobes, which is desirable for improving the overall efficiency of the reflector antenna. Additionally, the gap between the RHCP and LHCP patterns exceeds 15 dB at all frequencies, indicating proper performance of the circular polarization generated in each port.

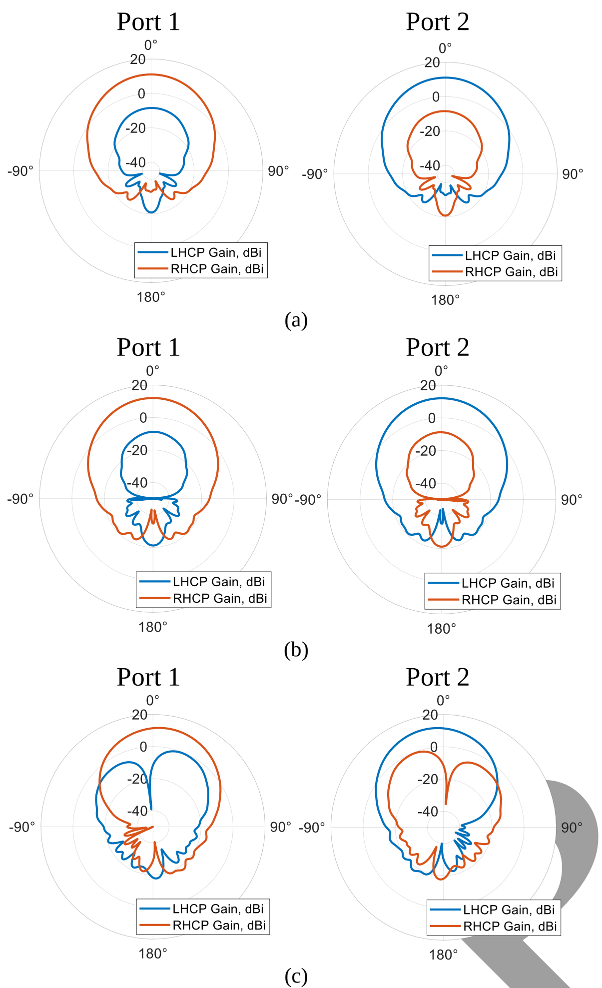

Fig. 9. RHCP and radiation patterns of the proposed antenna at (a) 1.65GHz, (b) 2.0 GHz, and (c) 2.3 GHz. The plots show the principal E-plane cut ($\phi = 0°$), with gain expressed in dBi and angle in degrees.

In the next step, the antenna is positioned at the focus of the 3-meter parabolic reflector, and its performance is evaluated in this configuration. It should be mentioned that all of the results of this part are simulation-based results. Due to the lack of a suitable outdoor or compact-range measurement facility for a 3-meter reflector, complete system measurements (feed + reflector) could not be performed. The simulated feed return loss in front of the 3-meter reflector is plotted. As demonstrated in Fig. 10, integration of the reflector structure does not introduce degradation of the return losses in Port 1 and Port 2, since the return loss in the range of 1.6 GHz to 2 GHz for both ports is lower than 10 dB.

The axial ratio in the presence of the reflector and at the location of the maximum antenna radiation (antenna boresight) is shown in Fig. 11. It can be seen that the axial ratio is also less than 3 dB in the range of 1.6 to 2.65 GHz. In other words, the antenna provides a circular-polarization bandwidth greater than 47% across the L and S bands.

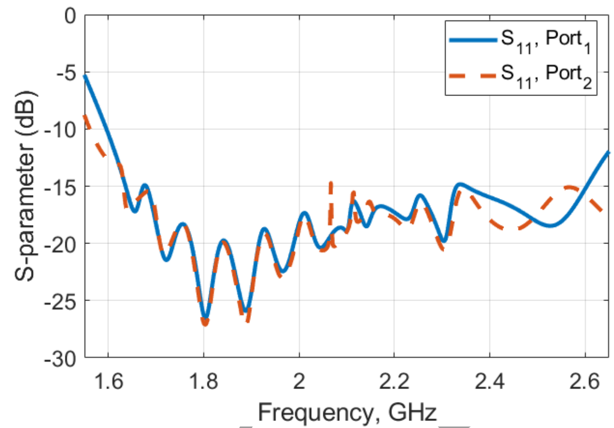

Fig. 10. The S-parameter of the proposed feed antenna in front of a 3-meter parabolic reflector.

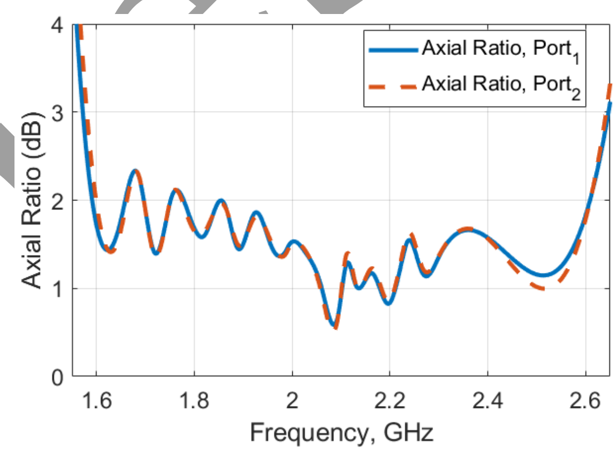

Fig. 11. The Axial Ratio of the proposed feed antenna in front of a 3-meter parabolic reflector.

The radiation pattern of the complete reflector antenna at 1.65 GHz, 2GHz, and 2.3 GHz is shown in Fig. 12. As can be seen, the antenna has a stable radiation pattern with very low sidelobe at all of the mentioned frequencies. The antenna realized gain at the three frequencies of 1.65, 2, and 2.3 GHz is 32, 33.6, and 34.8 dB, respectively. This is equivalent to an aperture efficiency of about 60% in all three frequencies. Also, the antenna sidelobe is obtained at these three frequencies as 30 dB, 27 dB, and 26 dB, respectively. This indicates a very low sidelobe in the proposed design.

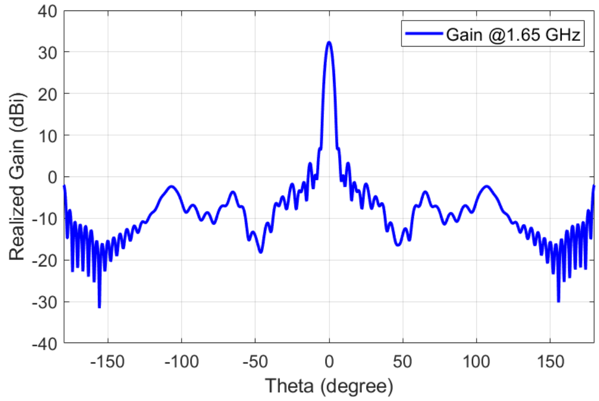

a)

b)

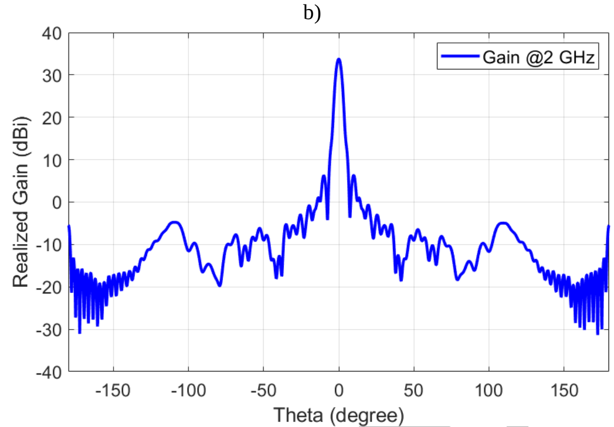

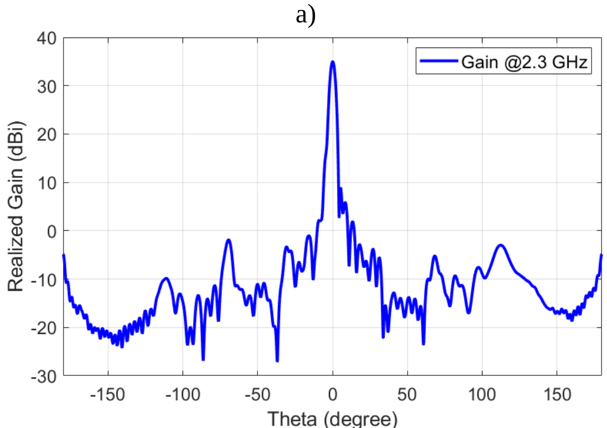

c)

Fig. 12. The radiation pattern of the complete reflector antenna at a) 1.65GHz, b) 2GHz, c) 2.3 GHz.

Table 6. Comparison of the proposed work with similar papers.

Ref	year	Center Freq. (GHz)	FBW (%)	3-dB AR FBW (%)	Peak Gain (dBi)	Aperture Efficiency (%)	Isolation (dB)	S_{11} (dB)	Reflector included
[19]	2011	L-band	3.9	3.9	N/A	N/A	>30	<-25	No
[20]	2016	Lband	1	1	16.2	N/A	>23	<-29	No
[21]	2009	X band	13	13	8	N/A	>20	<-19	No
[22]	2024	Ku band	33	16.7	14.9-16.4 Horn only	N/A	N/A	<-15	No
[24]	2022	Ka band	17.4	6.5	N/A	N/A	N/A	>-15	No
[30]	2022	W band	31.5	31.5	21.6	N/A	>32.5	>-20	No
This work	**2025**	**L/S**	**47.6**	**52.3**	32–34.8*	**>60**	>15	**>-15**	**Yes**

* Peak gain corresponds to the reflector-integrated antenna over the 1.6–2.6 GHz frequency range. N/A: Not available.

For a more detailed examination, the antenna gain in the range of 1.6 GHz to 2.6 GHz is plotted in Fig. 13. Based on this graph, it can be said that the antenna gain has an efficiency of better than 60% in the entire frequency range. The plot data in Fig. 10 to Fig. 13 confirm that the proposed reflector antenna remains viable for frequencies 1.6 to 2.6 GHz, based on an axial ratio below 3dB and return loss better than 10dB.

Next, the effect of adding a convex plate at the vertex of the reflector is investigated. This approach is used to compensate for the showing as described in the previous section. According to the plot data in Fig. 14, adding a convex plate at the reflector center considerably improved antenna gain at higher frequencies, while the antenna gain at lower frequencies did not change so much.

In Table 6, a brief comparison between this work and some recent papers about the septum horn antenna is presented. As can be seen, the proposed structure is capable of maintaining an axial ratio of less than 3dB in a

47% fractional bandwidth. In this respect, it is the most wideband structure presented so far. The designed structure has also been used as a feed for a 3-meter reflector antenna, and the radiation effects in the presence of the reflector antenna have been carefully studied.

By reviewing all the results obtained in this paper, a very wideband feed antenna has been presented to cover the two L and S frequency bands in a compact structure with high portability.

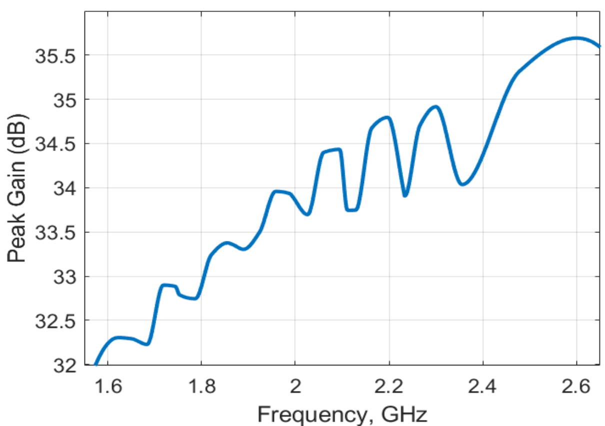

Fig. 13. Simulated Peak Gain of the reflector antenna over frequency

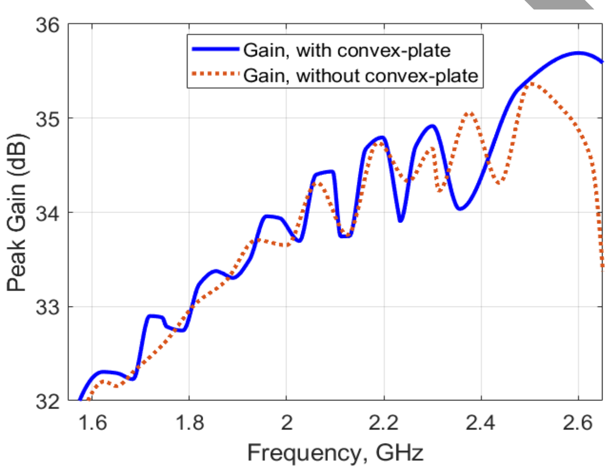

Fig. 14. Simulated Peak Gain of the reflector antenna with and without the convex plate at the antenna vertex.

4 Conclusion

This paper presents a wideband circularly polarized L/S-band septum horn feed antenna designed for satellite communication applications. The proposed design incorporates a corrugated horn antenna, a circular-to-rectangular waveguide converter, a wideband septum polarizer, and sloped waveguide outputs. Unlike conventional septum horns, this design features output ports extracted through optimal rectangular apertures from two sidewalls of the waveguide. These apertures connect to WR510 waveguides via sloped transition waveguides, enabling wideband circular polarization.

The antenna feeds a 3-meter reflector in a prime focus configuration, mounted at the focal point using a foldable multi-piece tripod for enhanced portability during transportation. To improve reflector efficiency, a convex plate is implemented at the reflector's apex. The final structure achieves an axial ratio below 3 dB across 1.6-2.6 GHz, representing a 47% fractional bandwidth centered at 2.1 GHz.

Additionally, the reflector demonstrates efficiency exceeding 60% with sidelobe levels better than 26 dB throughout the L/S band. A prototype of the feed antenna has been fabricated, and measurement results show good agreement with simulations.

Although the feed prototype was experimentally characterized, the full reflector-integrated antenna could not be measured due to the absence of suitable test facilities. Future work will focus on performing outdoor or compact-range measurements of the complete system and exploring further optimization of the feed geometry to improve bandwidth, reduce mass, and simplify fabrication.

Conflict of Interest

The authors declare no conflict of interest.

Author Contributions

Amir Mohammad Zaker: designed the antenna structure, performed simulations, conducted the analysis of the results, wrote the initial manuscript, and prepared figures. *Mohammad Bod*: Proposed the research concept, supervised the research, provided critical feedback, reviewed, and edited the manuscript. *Hamid Ghanizadeh Bafghi*: secured funding, managed project administration, conducted measurements, and contributed to data analysis. All authors discussed the results, reviewed the manuscript, and approved the final version.

Funding

This research has not received any funding.

Declaration of generative AI and AI-assisted technologies

During the preparation of this work, the authors used AI solely for grammatical and spelling corrections. After receiving AI-generated suggestions, the authors manually reviewed, selected, and edited all content to ensure accuracy and appropriateness. The authors take full responsibility for the final content of this manuscript.

References

[1] O. Kodheli et al., "Satellite Communications in the New Space Era: A Survey and Future Challenges," IEEE Communications Surveys & Tutorials, vol. 23, no. 1, pp. 70-109, 2021.

[2] K. Vasanth, K. G. Reddy, V. B. S. Datta, C. V. Narasimhulu, and K. Suman "Design of Ground Station Antennas for Tracking of LoRa based Satellites at 433MHz Amateur Frequencies," IEEE Int. Students’ Conf. Electr., Electron. Comput. Sci. (SCEECS), Bhopal, India, pp. 1–8, 2025.

[3] Y. Rahmat-Samii and A. C. Densmore, “Technology Trends and Challenges of Antennas for Satellite Communication Systems,” IEEE Trans. Antennas Propag., vol. 63, no. 4, pp. 1191–1204, Apr. 2015.

[4] Y. -B. Jung, A. V. Shishlov and S. -O. Park, "Cassegrain Antenna with Hybrid Beam Steering Scheme for Mobile Satellite Communications," IEEE Transactions on Antennas and Propagation, vol. 57, no. 5, pp. 1367-1372, May 2009.

[5] R. C. Gupta, S. K. Sagi and M. B. Mahajan, "Shaping of Offset Gregorian Reflector Antenna for Enhanced Performance during Beam-Steering in Multi-Position," IEEE Indian Conference on Antennas and Propagation (InCAP), Ahmedabad, India, 2019, pp. 1-5.

[6] Z. -Y. Zhang, Y. Zhao, N. -W. Liu, L. -Y. Ji, S. Zuo and G. Fu, "Design of a Dual-Beam Dual-Polarized Offset Parabolic Reflector Antenna,” IEEE Trans. Antennas Propag., vol. 67, no. 2, pp. 712-718, Feb. 2019.

[7] M. Bod, and F. Geran, "Design and Optimization of a Dual Polarized Hat Feed Reflector Antenna," Journal of Electrical and Computer Engineering Innovations (JECEI), vol. 10, no. 2, pp. 403-410.

[8] E. G. Geterud, J. Yang, T. Ostling and P. Bergmark, "Design and Optimization of a Compact Wideband Hat-Fed Reflector Antenna for Satellite Communications," IEEE Trans. Antennas Propag., vol. 61, no. 1, pp. 125-133, Jan. 2013.

[9] Amir Moallemizadeh, Reza Sarraf-Shirazi, and Mohammad Bod, "Design of a Novel Compact Cup Feed for Parabolic Reflector Antennas," Progress in Electromagnetics Research Letters, Vol. 64, 81-86, 2016.

[10] T. A. Milligan, T.A., Modern antenna design. John Wiley & Sons, 2005.

[11] Y. Liu, Z. Chen, C. Lan, B. Zhai and Y. Zheng, "Research and Design of Integration of L/S/X/Ka Multiband Feed," 2023 5th International Conference on Applied Machine Learning (ICAML), Dalian, China, pp. 426-432,2023.

[12] X. Ding, X. Yang, B. Feng, C. -Y. -D. Sim, S. Wu and K. L. Chung, "A Dual-Polarized Wideband Parabolic Reflector Antenna With High Aperture Efficiency and Low Sidelobe Level for L/S-Band Satellite Communications," IEEE Access, vol. 12, pp. 174859-174870, 2024.

[13] W. -F. Peng, W. -J. Ye and S. -H. He, "A novel dual-band and dual circular-polarization feed for paraboloidal reflector antenna," Int. Conf. Microw. Millimeter Wave Technol. (ICMMT), Shenzhen, China, pp. 1–3, 2012.

[14] K. W. Smart, R. Shaw, M. Bourne, M. Death, C. Granet and J. S. Kot, "Manufacture and Test of a Simultaneous S/X Feed System for a Satellite Ground Station," IEEE Asia-Pacific Microwave Conference (APMC), Brisbane, Australia, pp. 383-385, 2021.

[15] Aniket Gunjal, Ujwala Kshirsagar, "Feeding Analysis of Broadband CP Antenna: A Comprehensive Review", IEEE 16th International Conference on Computational Intelligence and Communication Networks (CICN), pp.81-88, 2024.

[16] Mohammad Bod, and Hamid Reza Hassani, "Multi-Band Circularly Polarized Slot Antenna for GPS, Bluetooth and WiMAX Bands," Progress In Electromagnetics Research C, Vol. 49, 171-178, 2014.

[17] R. Xu, J. -Y. Li and J. Liu, "A Design of Broadband Circularly Polarized C-Shaped Slot Antenna with Sword-Shaped Radiator and Its Array for L/S-Band Applications," IEEE Access, vol. 6, pp. 5891-5896, 2018.

[18] Z. Li, X. Ba, Z. Wang, X. Chen and S. Gao, "A Wideband Dual-Circularly Polarized Inverted Quad-Ridged Elliptical Waveguide Horn Antenna," IEEE Antennas Wireless Propag. Lett., vol. 23, no. 10, pp. 2850-2854, Oct. 2024.

[19] M. J. Franco, "A High-Performance Dual-Mode Feed Horn for Parabolic Reflectors with a Stepped-Septum Polarizer in a Circular Waveguide [Antenna Designer's Notebook]," IEEE Antennas and Propagation Magazine, vol. 53, no. 3, pp. 142-146, June 2011.

[20] M. Mrnka, M. Pavlovic and Z. Raida, "Antenna Range Illuminator Based on a Septum Polarizer and a Dual-Mode Horn [Measurements Corner]," IEEE Antennas and Propagation Magazine, vol. 58, no. 4, pp. 82-86, Aug. 2016.

[21] C. Kumar, V. V. Srinivasan, V. K. Lakshmeesha and S. Pal, "Novel Dual Circularly Polarized Radiating Element for Spherical Phased-Array Application," IEEE Antennas and Wireless Propagation Letters, vol. 8, pp. 826-829, 2009.

[22] C. Dong et al., "Dual Circularly-Polarized Septum Antenna Array Based on an Air-Filled Dual-Mode Feeding Network," IEEE Trans. Antennas Propag., vol. 72, no. 3, pp. 2938-2943, March 2024.

[23] B. P. Kumar, K. Gopal, P. V. Sitaraman, C. Sriharha and V. S. Kumar, "High Efficiency Small Reflector Antenna Design for Satellite Application," IEEE Wireless Antenna and Microwave Symposium (WAMS), Visakhapatnam, India, pp. 1-4, 2024.

[24] Y. Fu, K. Y. Chan and R. Ramer, "A 3D-Printed Horn Antenna with Integrated Septum and Circular-Polarized Radiation," IEEE MTT-S International Microwave Workshop Series on Advanced Materials and Processes for RF and THz Applications (IMWS-AMP), Guangzhou, China, pp. 1-3, 2022.

[25] C. Shu et al., "A Wideband Dual-Circular-Polarization Horn Antenna for mmWave Wireless Communications," IEEE Antennas Wireless Propag. Lett., 18, no. 9, pp. 1726-1730, Sept. 2019.

[26] S. Arora, P. V. Sitaraman, B. Sandhya Reddy, V. S. Kraanthi, C. Sriharsha and V. Senthil Kumar, "Dual Polarized Global Coverage Horn Antenna for CDMA based Satellite TTC Applications," IEEE Indian Conference on Antennas and Propogation (InCAP), Hyderabad, India, pp. 1-4,2018.

[27] H. Cho, K. -Y. Park, C. -M. Lim and H. -W. Son, "Design and Implementation of an X-Band Horn Antenna With a Metamaterial Lens Using 3D Printing Technology," IEEE Access, vol. 12, pp. 17773-17781, 2024.

[28] Wang, Z. Xu, Z. Wang, X. Zheng and Y. Rahmat-Samii, "Development of a Low-Cost Lightweight Advanced K-Band Horn Antenna With Charge-Programmed Deposition 3-D Printing," IEEE Antennas Wireless Propag. Lett., vol. 22, no. 8, pp. 1917-1921, Aug. 2023.

[29] I. Kim, J. M. Kovitz and Y. Rahmat-Samii, "Sigmoid profiled septum: Evaluation of the parabolic reflector with the septum feed horn," IEEE Antennas and Propagation Society International Symposium (APSURSI), Orlando, FL, USA, 2013.

[30] C. Shu et al., "Wideband Dual-Circular-Polarization Antenna with High Isolation for Millimeter-Wave Wireless Communications," IEEE Trans. Antennas Propag., vol. 70, no. 3, pp. 1750-1763, March 2022.

[31] P.-S. Kildal, Foundations of Antenna Engineering: A Unified Approach for Line-of-Sight and Multipath. Norwood, MA, USA: Artech House, 2015.

[32] Dubrovka, F.F., Piltyay, S.I., Dubrovka, R.R. et al. "Optimum Septum Polarizer Design for Various Fractional Bandwidths," Radio electron. Commun. Syst. 63, 15–23, 2020.

[33] C. Granet and G. L. James, "Design of corrugated horns: a primer," IEEE Antennas Mag., vol. 47, no. 2, pp. 76-84, April 2005.

Biographies (All Authors)

Amir Mohammad Zaker recently completed his Bachelor's degree in Electrical Engineering, specializing in Telecommunication, from Shahid Rajaee University (SRU). His research interests encompass Satellite Communications, Antennas and Propagation Analysis, Radar and Remote Sensing Systems, and Digital Signal Processing and Algorithms.

Mohammad bod was born in Tehran, Iran, in 1986. He received a Ph.D. degree in electrical engineering from the Amirkabir University of Technology University, Tehran, in 2018. From 2019 to 2021, he was a Post-Doctoral Researcher at Amirkabir University with a fellowship awarded by the Iran National Science Foundation (INSF). He is currently an Assistant Professor at the ElectricalEngineering Department, Shahid Rajaee Teacher Training University, Tehran. He has authored or co-authored 30 journal papers and two Persian books. His research interests include phased array radar, antenna and passive microwave component design, and numerical methods in electromagnetic.

• **Email:** Mohammadbod@sru.ac.ir

Hamid G. Bafghi received the B.Sc. degree from Shahid Beheshti University,Tehran, Iran, in 2008 and the M.Sc. and Ph.D. degrees in electrical engineering from Shahed University, Tehran, Iran, in 2011 and 2016, respectively. He hasbeen a Post-Doctoral Research Fellow with the Wireless Research Laboratory, Sharif University of Technology, Tehran, since 2016. His research interests include information theory and its applications in security, privacy, energy harvesting, cognitive communications, molecular communications, and machine learning.